# Cation and vacancy distribution in an artificially oxidized natural spinel

GIORGIO MENEGAZZO

Liceo Scientifico I. Nievo, Padova, Via Barbarigo 38, 35141 Padova, Italy

SUSANNA CARBONIN AND ANTONIO DELLA GIUSTA

Dipartimento di Mineralogia e Petrologia, Università di Padova, Corso Garibaldi 37, 35122 Padova, Italy

**Abstract**

During research on the influence of temperature on cation partitioning in natural Mg–Al–$Fe^{2+}$–$Fe^{3+}$ spinels, some crystals were accidentally oxidized during heat treatment. The oxidation product, studied by means of single-crystal X-ray diffraction, turned out to be a phase retaining the *Fd3m* parent spinel structure, but with cell edge $a$ and oxygen coordinate $u$ considerably smaller than the parent ones ($a \sim 8.087$ as compared with $\sim 8.111$ Å; $u \sim 0.2609$ *vs.* 0.2617–0.2636) and with vacant sites due to oxidation.

Assuming that the oxidation process must occur due to the addition of oxygen to the crystal boundary as cations are being preserved and rising in total valence, the site population was determined and compared with that of untreated and heated samples. It was found that, on oxidation, a charge enrichment in the tetrahedral site T had occurred, this phenomenon following that observed during heating at increasing temperatures also in other spinel series. This continuity was always in the direction of an increase in random charge distribution. Cation vacancies produced during oxidation were restricted to the octahedral site M.

Examination of bulk sections by reflected light microscopy showed a few hematite lamellae as inclusions in the oxidized samples, not detectable by microprobe analysis or single-crystal structural refinement. However, hematite played a marginal part in oxidation. Vacancy-oxygen distances in oxidized spinels were determined from experimental data in the literature.

KEYWORDS: spinel, oxidation, vacancies, site population.

## Introduction

RESEARCH was undertaken on a Mg–Al–Fe spinel from the Balmuccia peridotite (Italian Western Alps), with the aim of studying cation distribution in various conditions. Cation partitioning was calculated by applying a mathematical model to the experimental data obtained from single-crystal X-ray diffraction and electron microprobe analysis.

This study was carried out in three phases:

*Untreated samples*: comparison between calculated cation distributions in single crystals and those observed on powders from Mössbauer spectroscopy. The satisfactory agreement found proved the reliability of the model and the assumptions made, at least in the samples studied. In the examined spinels, $Fe^{2+}$ and $Fe^{3+}$ were virtually ordered, in T and M sites respectively.

*Site population variations*: analysis of crystals heated at various temperatures for various durations and then quenched. Thermal runs and quenching maintained substantially ordered distribution of $Fe^{2+}$ and $Fe^{3+}$ up to $\sim 990$°C and produced continuous $^{[4]}Mg$-$^{[6]}Al$ exchange. Between 990 and 1150°C, the previous order of $Fe^{2+}$-$Fe^{3+}$ appeared to change slightly towards an increase in $^{[6]}Fe^{2+}$; $^{[6]}Mg$ and $^{[4]}Al$ disorder reached its maximum at the highest temperature. After quenching from this temperature, $Fe^{2+}$ still resided mainly in the T site.

*Determination of cation distribution* in some samples which underwent oxidation during the above experiments.

*Mineralogical Magazine, June 1997, Vol. 61, pp. 411–421*
© *Copyright the Mineralogical Society*

The first two phases of this research, which were recently published (Carbonin *et al.*, 1996; Della Giusta *et al.*, 1996), report spinel characteristics (occurrence, homogeneity) and experimental techniques in more detail.

## Data collection

Rock sample TS2 comes from a suite of websteritic dykes crossing a peridotite of mainly lherzolitic composition in the Ivrea-Verbano area, Italian Western Alps (Comin-Chiaramonti *et al.*, 1982; Pizzolon, 1991).

The homogeneity of TS2 spinels was tested by microprobe in 103 randomly chosen points of one thin section. Whereas single grains showed sufficiently good homogeneity, their chemical composition was quite different from grain to grain, above all as regards Cr content. Several crystals extracted from the same hand-picked specimen had to be examined before seven (A–G) suitable for single-crystal data collection could be identified. They shared both similar cell parameters and Cr content — the latter being much lower than average on ~100 analysed points.

The crystals were mounted on a STOE AED4 single-crystal diffractometer with monochromatized Mo-$K\alpha$ radiation. Unit cell parameters $a$ were always obtained with the same standard program of the diffractometer. Intensities were collected in the $\omega$ - $2\theta$ scan mode up to $2\theta \cong 100°$ and used for crystal structural refinement with the SHELX-93 program (Sheldrick, 1993). Corrections for absorption and background were performed following North *et al.* (1968) and Blessing *et al.* (1972) respectively. Structural refinements were carried out in the $Fd3m$ space group (with origin at $\bar{3}m$), since no evidence of different symmetry appeared. Refined parameters were: scale factor, secondary extinction coefficient, oxygen coordinate $u$, tetrahedral and octahedral site occupancies, and displacement parameters. Two scattering curves, Mg *vs.* Fe in the T site and Al *vs.* Fe in the M site, were assigned to sites involved in isomorphous replacements, with the constraint of full site occupancy and equal displacement parameters. No constraints were imposed by chemical analyses.

After X-ray data collection, chemical analysis was performed on the polished surface of the same single crystal used for the XRD study. Composition was obtained on the Cameca/Camebax electron microprobe at the Department of Mineralogy and Petrology of the University of Padova. Analyses were performed at 15 kV and 15 nA sample current, using only the WDS method. X-ray counts were converted into oxide weight percentages using a PAP correction program provided by Cameca. At least five point analyses were performed on each crystal.

## Model used for cation distribution calculation

Cation distribution was calculated in order to find the best fit for the experimental results. The necessary data obtained by the methods and procedures described above and considered with their errors, are:

ten atomic frequencies $X_{obs,j}$ per formula unit (f.u.) obtained from microprobe analysis;

structural refinement parameters:

$$a = \frac{8}{11\sqrt{3}}\left[5(\mathrm{T}-\mathrm{O}) + \sqrt{33(\mathrm{M}-\mathrm{O})^2 - 8(\mathrm{T}-\mathrm{O})^2}\right] \quad (1)$$

where T–O and M–O are the bond distances;

$$u = \frac{0.75R - 2 + \sqrt{\frac{33}{16}R - 0.5}}{6(R-1)} \quad (2)$$

where $R = (\mathrm{M}-\mathrm{O})^2/(\mathrm{T}-\mathrm{O})^2$;

$e^-(\mathrm{T}) = \Sigma X_{\mathrm{T},i}Z_i$ and $e^-(\mathrm{M}) = \Sigma X_{\mathrm{M},i}Z_i$,

where $X_{\mathrm{T\ or\ M},i}$ are the atomic fractions in T and M sites, and $Z_i$ the atomic number of the actual species in the spinel studied.

The mathematical model used for calculations was based on the assumption that $\mathrm{T}-\mathrm{O} = \Sigma R_{\mathrm{T},i}X_{\mathrm{T},i}$ and $\mathrm{M}-\mathrm{O} = 1/2\Sigma R_{\mathrm{M},i}X_{\mathrm{M},i}$, where $R_{\mathrm{T\ or\ M},i}$ are pure bond lengths relative to the various species, presumed to be known and constant (Hill *et al.*, 1979). Substituting these expressions in equations (1) and (2) gives $a$ and $u$ as functions of $X_i$, the atomic fractions in the two sites. There are then $N = 18$ quantities (19, in the case of vacancies) which can be expressed through $X_{\mathrm{T\ or\ M},i}$: $a$; $u$; $e^-(\mathrm{T})$; $e^-(\mathrm{M})$; number of cations both per f. u. and in T and M sites (3, 1 and 2 respectively); number of charges for the balance; and 10 atomic proportions $X_{obs,j}$ from microprobe analysis (plus, in the case of oxidized samples, the number of vacancies). Moreover, minor cations were assumed to be assigned to only one site, on the basis of their general site preference: $Si^{4+}$, $Mn^{2+}$ and $Zn^{2+}$ to the T site; $Cr^{3+}$, $Ni^{2+}$ and $Ti^{4+}$ to the M site. Therefore, each sample was characterized by the 14 parameters (16 in the case of vacancies) $X_{\mathrm{T\ or\ M},i}$ (6 for minor elements plus $2.\times 4$ or $2\times 5$ for major elements and vacancies) to be determined.

The best estimate of these parameters was assumed to be the one minimizing the sum:

$$R(X_i) = \sum_{j=1}^{N}\left[\frac{O_j - C_j(X_i)}{\sigma_j}\right]^2 \quad (3)$$

where $O_j$ is a quantity observed, $C_j(X_i)$ the same quantity calculated by means of parameters $X_i$, and $\sigma_j$ the standard deviation of the observed quantity $O_j$.

Minimization was performed by means of the MINUIT program (James and Roos, 1975). No

constraints were imposed, even on the equality between $X_{obs,j}$ and $X_{T,j} + X_{M,j}$ or the assignment of vacancies or major cations to one site. The sum of the $N$ (18 or 19) residuals of equation (3) turned out to be homogeneous in all samples and typically $\sim 2$; thus, in any case, cation distributions were found to be in very satisfactory agreement with the experimental data.

The cation-to-oxygen distances used (Å) are those already published ($R_T$: Mg–O = 1.965, $Fe^{2+}$–O = 1.996, $Fe^{3+}$–O = 1.891, Al–O = 1.767, Mn–O = 2.040, Si–O = 1.652, Zn–O = 1.966; $R_M$: Mg–O = 2.095, $Fe^{2+}$–O = 2.138, $Fe^{3+}$–O = 2.020, Al–O = 1.909, Cr–O = 1.996, Ni–O = 2.076, Ti–O = 1.985). Instead, the vacancy-to-oxygen distances were first obtained from the experimental data of Kullerud *et al.* (1969) on 'kenotetrahedral' and 'kenooctahedral magnetites'. These distances were then refined from the data on 27 non-stoichiometric Mg–Al synthetic spinels reported by Lucchesi and Della Giusta (1994) and were $R_{T,\square} = 2.229$ and $R_{M,\square} = 2.105$ Å.

### Sample oxidation

In order to study the variations in site population due to temperature, the crystals were sealed in $SiO_2$ tubes 2 mm in diameter, containing an iron-wüstite buffer wrapped in platinum foil to prevent reaction between iron and silica, and placed in a vertical furnace. However, in thermal runs at 1150°C after $\sim 10$ h and at 700°C after 30 days, incipient recrystallization of the tube occurred and air entered through the silica grain boundaries, with consequent oxidation of spinel. The oxidized crystals (TS2B6, C5, D4), heated at 680°C for four months and then quenched in water, were dark brown in colour and appeared somewhat metallic on the surface, with respect to the unoxidized parents, which were always green and quite translucent.

A preliminary examination of these oxidized spinels by single-crystal diffractometer showed that the reflections were of very good quality and indicated a cubic face-centred Bravais lattice, no violation being observed. A data collection procedure with profile fitting was selected: preliminarily, a set of $\sim 50$ reflections, including $\{hhh\}$ and covering as wide a range of $2\theta$ as possible, was used to best determine the shape of the profile and the parameters describing its width (Clegg, 1981). A quarter of the reciprocal space was then examined, so that up to 12 equivalent reflections of the general form $\{hkl\}$ were measured. After correction for Lorentz and polarization effects and isotropic secondary extinction, a set of $\sim 160$ observed structural factors $Fo_{hkl}$ was obtained from each crystal.

The crystallographic parameters provided by structural refinement were quite different from those of untreated and heated samples, in particular as regards cell edges, oxygen coordinates and extinction coefficients (*Ext*) (see Table 1, from data already published in Della Giusta *et al.*, 1996). The latter parameter decrease was probably caused by more crystal imperfections due to the vacancies, as suggested by Colombo *et al.* (1964*a*).

After X-ray data collection, electron microprobe analyses were performed on these crystals. In TS2C5 and D4, the first section to be analysed was not deep but quite near the surface. Although points analysed right on the borderline revealed much higher FeO contents than in the unoxidized sample, points inside but still on the rim and near the previous ones showed a significant depletion in the same oxide. After a second polishing, which revealed an equatorial zone, the analysed points no longer showed significant differences in FeO content with respect to the unoxidized sample. Instead, approximately 30 points of crystal TS2B6, which was first analysed close to the equatorial zone, did not show significant differences from analysis before oxidation. This indicates that iron atoms had migrated towards the surface, although they came from the nearest underlying layers. It may therefore be concluded that the most representative analysis of the oxidized sample was not significantly different from that of the parent spinel, except for some inhomogeneous zones near the surface where some iron loss occurred.

During crystal polishing for microprobe analysis, examination of one bulk section by reflected light microscopy showed some inclusions of hematite, identified by morphology, reflectance, colour and anisotropy. They were particularly evident when the lamellae were needle-like in shape, $\sim 0.5\ \mu m \times 5\ \mu m$, and oriented only in particular directions (probably $\{111\}$) of the host crystal (Davis *et al.*, 1968; Fleet and Arima, 1985). In one particularly thin crystal, they were detected in transmitted light as pseudo-hexagonal in shape and so translucent as to appear characteristically orange-red in colour.

Microprobe analyses of spinel crystals with hematite inclusions, although performed with a defocussed electron beam, failed to reveal the expected increase in total iron contents, as compared to inclusion-free spinel compositions. The lamellae were detectable only by means of an Fe-$K\alpha$ scanning picture. An FeO content significantly higher than the average was measured by means of a highly focussed beam just over these inclusions. Similarly, X-ray data collection failed to reveal any contribution of hematite to the spinel $\{hhh\}$ reflections. Again, although there were some indications of the presence of hematite seeds in untreated samples, they could not be detected even by Mössbauer spectroscopy.

In conclusion, hematite formation was a quantitatively secondary phenomenon in oxidation: the role

TABLE 1. Crystal data in natural unheated, heated, and oxidized spinels

| Sample | $T$ (°C) | $t$ | $a$ (Å) | $u$ | *Ext.'* | T–O (Å) | M–O (Å) | $e^-$(T) | $e^-$(M) | $e^-_{total}$ |
|---|---|---|---|---|---|---|---|---|---|---|
| TS2B1 | unheat. | | 8.1108 (4) | 0.26361 (7) | 8.77 | 1.9472 (10) | 1.9237 (5) | 15.28 (13) | 13.40 (6) | 42.08 |
| TS2B2 | 695 | 110 m | 8.1113 (3) | 0.26359 (7) | 9.49 | 1.9471 (10) | 1.9239 (5) | 15.38 (12) | 13.33 (6) | 42.04 |
| TS2B3 | 915 | 60 m | 8.1089 (4) | 0.26215 (9) | 10.35 | 1.9263 (13) | 1.9337 (7) | 15.40 (13) | 13.41 (6) | 42.22 |
| TS2B6§ | 680 | 120 d | 8.0875 (9) | 0.26091 (7) | 2.26 | 1.9038 (10) | 1.9377 (6) | 14.50 (10) | 13.24 (6) | 40.98 |
| TS2C1 | unheat. | | 8.1113 (4) | 0.26354 (8) | 7.67 | 1.9464 (11) | 1.9243 (6) | 15.33 (14) | 13.41 (7) | 42.15 |
| TS2C2 | 730 | 46 h | 8.1105 (3) | 0.26307 (8) | 8.46 | 1.9396 (11) | 1.9275 (6) | 15.60 (13) | 13.39 (6) | 42.37 |
| TS2C5§ | 680 | 120 d | 8.0891 (6) | 0.26107 (8) | 3.02 | 1.9064 (11) | 1.9369 (6) | 14.61 (11) | 13.28 (6) | 41.17 |
| TS2D1 | unheat. | | 8.1143 (3) | 0.26361 (7) | 9.02 | 1.9481 (10) | 1.9245 (5) | 15.44 (13) | 13.51 (6) | 42.46 |
| TS2D2 | 650 | 31 d | 8.1138 (3) | 0.26349 (7) | 7.92 | 1.9463 (10) | 1.9252 (5) | 15.60 (11) | 13.47 (5) | 42.55 |
| TS2D3 | 675 | 24 d | 8.1151 (3) | 0.26348 (7) | 8.56 | 1.9464 (10) | 1.9256 (5) | 15.61 (11) | 13.47 (5) | 42.54 |
| TS2D4§ | 680 | 120 d | 8.0850 (9) | 0.26073 (7) | 2.56 | 1.9007 (10) | 1.9384 (6) | 14.29 (11) | 13.22 (6) | 40.74 |
| TS2G1 | unheat. | | 8.1136 (3) | 0.26367 (6) | 5.93 | 1.9488 (8) | 1.9239 (4) | 15.40 (11) | 13.38 (5) | 42.16 |
| TS2G2 | 1150 | 3 m | 8.1121 (4) | 0.26176 (8) | 4.81 | 1.9216 (11) | 1.9373 (6) | 15.56 (11) | 13.50 (6) | 42.55 |
| TS2G3 | 1150 | 100 m | 8.1107 (4) | 0.26168 (8) | 8.26 | 1.9201 (11) | 1.9376 (6) | 15.48 (12) | 13.45 (6) | 42.39 |

Notes: In sample list, last number refers to various experiments on same crystal; penultimate letter refers to different crystals from TS2 sample.
§ Oxidized samples; *Ext.'* = $Ext \times 10^3$. Data from Della Giusta *et al.*, 1996.

of the seeds may have consisted in catalyzing this process, as suggested by Colombo *et al.* (1964*b*).

### Mechanism of oxidation

The adopted oxidation model is based on the assumption that free oxygen at the surface of the crystal is adsorbed into the framework and ionized by $Fe^{2+}$ atoms, according to the reaction (O'Reilly and Banerjee, 1967):

$$Fe^{2+} + \tfrac{1}{2}zO \rightarrow zFe^{3+} + (1-z)Fe^{2+} + \tfrac{1}{2}zO^{2-},$$

where degree of oxidation $z$ is the ratio between the number per f.u. of oxidized $Fe^{2+}$ ions and the initial number, $Fe_0^{2+}(0 \leqslant z \leqslant 1)$. Cations from inside the crystal then diffuse through the lattice and combine with anions to form new cells at the surface of the crystal, the continuous layer of $\alpha$-$Fe_2O_3$ on the surface not preventing further oxidation inside the crystal (Feitknecht and Gallagher, 1970). Moreover, it is assumed that other possible concurrent phenomena are negligible.

As the increment in the number of oxygens per f.u. is $\Delta O = \frac{1}{2}zFe_0^{2+}$, the ratio between the number of oxygens of the whole crystal before and after oxidation, $N_0oxygens$ and $Noxygens$ respectively, is:

$$k = \frac{N_0oxygens}{Noxygens} = \frac{4}{4+\Delta O} = \frac{4}{4+\frac{1}{2}zFe_0^{2+}}$$

Since the total number of cations in the whole crystal $Nc$ is preserved:

$$Nc = \frac{N_0oxygens}{4}n_0 = \frac{Noxygens}{4}n \qquad (4)$$

where $n_0$ and $n$ are the numbers of cations per 4 oxygens before and after oxidation, respectively ($n_0 = 3$).

From equation (4) it follows that:

$$n = \frac{N_0oxygens}{Noxygens}n_0 = kn_0 = 3\frac{4}{4+\frac{1}{2}zFe_0^{2+}}$$

Thus, the total number of cations per f.u., and consequently also each atomic fraction, must be rescaled, because the initial number of cations is redistributed over an increased number of cells. Therefore, if the initial atomic fractions are $Fe_0^{2+}$, $Fe_0^{3+}$, $X_{0,i}$, after oxidation they become:

$$X_{Fe^{2+}} = k(Fe_0^{2+} - zFe_0^{2+}) = k(1-z)Fe_0^{2+} \qquad (5)$$

$$X_{Fe^{3+}} = k(Fe_0^{3+} + zFe_0^{2+}) \qquad (6)$$

$$X_i = kX_{0,i} \qquad (7)$$

Moreover, vacancies $\square$ form in the crystal, and their number $X_\square$ per f.u. is:

$$X_\square = n_0 - n = n_0(1-k) = 3\left(1 - \frac{4}{4+\frac{1}{2}zFe_0^{2+}}\right) = 3\frac{\frac{1}{2}zFe_0^{2+}}{4+\frac{1}{2}zFe_0^{2+}} \qquad (8)$$

As for the total number of cations $Nc$, the total number of electrons $Ne^-$ of the same cations in the whole crystal is also preserved. Therefore, as in equation (4):

$$Ne^- = \frac{N_0oxygens}{4}e_0^- = \frac{Noxygens}{4}e^- \qquad (9)$$

where $e_0^-$ and $e^-$ are the numbers of electrons per f.u. before and after oxidation, respectively.

From equation (9), and also using equation (8), it follows that:

$$e^- = \frac{N_0oxygens}{Noxygens}e_0^- = ke_0^- = \frac{n}{n_0}e_0^- = \frac{3-X_\square}{3}e_0^- \qquad (10)$$

So the number of electrons per f.u. decreases on oxidation, and the number of vacancies can be calculated from this variation. In fact, equation (10) gives:

$$X_\square = 3\left(1 - \frac{e^-}{e_0^-}\right) \qquad (11)$$

As the number of vacancies is also correlated to degree of oxidation $z$ and to $Fe_0^{2+}$, equation (8) gives:

$$z = 8\frac{X_\square}{(3-X_\square)Fe_0^{2+}} \qquad (12)$$

Therefore, once the number of electrons per f.u. before and after oxidation and $Fe_0^{2+}$ are known, equations (11) and (12) provide both the number of vacancies and the degree of oxidation.

Errors in quantities (11) and (12) may be calculated from:

$$\sigma_\square = \frac{3}{e_0^-}\sqrt{\sigma_{e^-}^2 + \left(\frac{e^-}{e_0^-}\right)^2\sigma_{e_0^-}^2} \qquad (13)$$

$$\sigma_z = \frac{8}{(3-X_\square)Fe_0^{2+}}\sqrt{\frac{9(Fe_0^{2+})^2}{[(3-X_\square)Fe_0^{2+}]^2}\sigma_\square^2 + \frac{X_\square^2}{(Fe_0^{2+})^2}\sigma_{Fe_0^{2+}}^2} \qquad (14)$$

## Crystallographic data in unoxidized and oxidized samples

### *Electrons from X-ray structural refinements*

Electrons calculated from site-occupancy refinements decrease in all three samples after oxidation, from 42.30 to 40.96 on average. A reasonable estimate from equations (11) and (13) is $X_{\square} = 0.095 \pm 0.018$. In sample TS2D, the $e^-/e_0^-$ ratio is slightly lower than in the other samples, so that a slightly larger number of vacancies is to be expected. An analogous estimate of the degree of oxidation derived from equations (12) and (14) for the mean of the three samples ($Fe_0^{2+} \cong 0.225$) gives $z$ slightly higher than 1, with an error of 0.2, so that this oxidation may reasonably be regarded as total. Further confirmation of this comes from the striking coincidence between the numbers of electrons which can be calculated from equation (10) for $z = 1$, and those effectively observed from site occupancy refinements, in all three samples.

### *Electrons in T and M sites*

The decrease in number of electrons after oxidation is not homogeneously distributed: $e^-$(M) is almost unchanged, whereas a loss of $\sim 1e^-$ occurs in the T site. This suggests that: (i) vacancies are restricted to the T site; (ii) more complex exchanges occurred between T and M sites, in which lighter atomic species migrated from M to T.

However, mechanism (i) alone is not sufficient to explain the phenomenon, because cations already residing in the T site cannot have maintained their ratios unchanged. If this is so, on average for the three samples, $e^-(T)$ should be $(1 - X_{\square}) \times e_0^-(T) \cong (1 - 0.095) \times 15.48 \cong 14.02$, whereas the value is in fact $e^-(T) \cong 14.47$. Therefore, it may reasonably be expected that light atoms occupy most of the T sites.

### *Cell edges*

The $a$ parameter decreases with increasing vacancies, as also observed in other spinels (Viertel and Seifert, 1979; Navrotsky *et al.*, 1986; Basso *et al.*, 1991; Lucchesi and Della Giusta, 1994). A decrease in cell edge with vacancies is also described by Kullerud *et al.* (1969) in magnetites, when they are restricted to the M site.

### *Oxygen parameter*

The oxygen coordinate in the oxidized samples is diminished, suggesting complex exchanges of cations between sites, as already described in defect-free natural spinels (Princivalle *et al.*, 1989). In particular, the already observed relationship between the decrease in $u$ and the charge increase in the T site (Della Giusta *et al.*, 1996) suggests that, in this case too, the phenomenon is to be related to the increase in trivalent cations in the tetrahedron.

### *T–O and M–O bond lengths*

T–O undergoes a significant decrease, the lowest values being found in sample TS2D4, which also has the lowest $a$ value. This confirms that the ratio between tetrahedral cations does change and eliminates any doubt about vacancies in this site: if there were any vacancies, the T–O bond length would increase, due to longer distances in vacant sites than in any of the occupied ones. The M–O bond length maintains similar values to those of crystals heated to the highest temperature (1150°C). As vacancies are restricted to this site, more cations with smaller ionic radii than in the highest-temperature crystals are expected to counterbalance vacancies here, which in this site too have greater radii (2.105 Å, as opposed to 1.909, 2.020, 2.095 Å for $^{[6]}Al$, $^{[6]}Fe^{3+}$, $^{[6]}Mg$ respectively).

### *Conclusions*

The crystallographic data indicate that, in the T site:

there are no vacancies;

lighter atoms, including several trivalent atoms, occupy the site.

## Cation distribution calculation in oxidized samples

The chemical formulae of the three oxidized samples were obtained from those before oxidation by using equations (5) – (8), for $z$ varying from 0.0 to 1.0 with a step of 0.1. The minimum of equation (3) was sought for each formula thus obtained. In all three cases, it was found that the goodness of fit, which was inverse to the sum of the residuals, improved continuously for $z$ from 0.0 to 1.0. Therefore, the experimental data fit the hypothesis of total oxidation better, as already suggested by the decrease in number of total electrons.

The chemical formulae on the basis of four oxygens and the best cation distributions, relative to $z = 1$, are listed in Table 2 which, for comparison, also shows the distributions of some unoxidized samples already published in Della Giusta *et al.* (1996).

## Discussion of cation distribution and comparison with that of parent unoxidized spinel

In comparing cation distribution before and after oxidation, it must be recalled that, although the cation fraction in oxidized samples is diminished by a factor of $k$ (equations (5)–(8)), comparison between

TABLE 2. Cation distributions in TS2 and comparison between observed and calculated structural parameters: obs. from structural refinement, calc. from cation distribution

| Sample | Site | Al | $Fe^{2+}$ | $Fe^{3+}$ | Mg | Mn | Si | Zn | Cr | Ni | Ti | □ | | $a$ | $u$ | $e^-$(T) | $e^-$(M) |
|---|---|---|---|---|---|---|---|---|---|---|---|---|---|---|---|---|---|
| TS2B 1 | T | 0.1222 | 0.2169 | 0.0000 | 0.6552 | 0.0021 | 0.0011 | 0.0025 | | | | | obs. | 8.1108 | 0.26361 | 15.28 | 13.40 |
| | M | 1.8147 | 0.0006 | 0.0477 | 0.1170 | | | | 0.0127 | 0.0068 | 0.0005 | | calc. | 8.1108 | 0.26361 | 15.23 | 13.38 |
| 2 | T | 0.1201 | 0.2167 | 0.0089 | 0.6486 | 0.0021 | 0.0011 | 0.0024 | | | | | obs. | 8.1113 | 0.26359 | 15.38 | 13.33 |
| | M | 1.8158 | 0.0000 | 0.0394 | 0.1248 | | | | 0.0127 | 0.0068 | 0.0005 | | calc. | 8.1113 | 0.26359 | 15.35 | 13.32 |
| 3 | T | 0.2280 | 0.2156 | 0.0000 | 0.5506 | 0.0021 | 0.0011 | 0.0025 | | | | | obs. | 8.1089 | 0.26215 | 15.40 | 13.41 |
| | M | 1.7061 | 0.0051 | 0.0504 | 0.2183 | | | | 0.0127 | 0.0068 | 0.0005 | | calc. | 8.1089 | 0.26215 | 15.32 | 13.37 |
| 6§ | T | 0.2497 | 0.0000 | 0.1509 | 0.5935 | 0.0021 | 0.0011 | 0.0025 | | | | 0.0000 | obs. | 8.0875 | 0.26091 | 14.50 | 13.24 |
| | M | 1.6421 | 0.0000 | 0.1045 | 0.1527 | | | | 0.0123 | 0.0067 | 0.0005 | 0.0809 | calc. | 8.0880 | 0.26090 | 14.44 | 13.20 |
| | Total | 1.8918 | 0.0000 | 0.2555 | 0.7463 | 0.0021 | 0.0011 | 0.0025 | 0.0123 | 0.0067 | 0.0005 | 0.0809 | | | | | |
| TS2D 1 | T | 0.1270 | 0.2187 | 0.0004 | 0.6481 | 0.0021 | 0.0011 | 0.0025 | | | | | obs. | 8.1113 | 0.26354 | 15.33 | 13.41 |
| | M | 1.8079 | 0.0000 | 0.0490 | 0.1231 | | | | 0.0127 | 0.0068 | 0.0005 | | calc. | 8.1113 | 0.26354 | 15.27 | 13.38 |
| 2 | T | 0.1597 | 0.2251 | 0.0062 | 0.6032 | 0.0022 | 0.0010 | 0.0026 | | | | | obs. | 8.1105 | 0.26307 | 15.60 | 13.39 |
| | M | 1.7736 | 0.0000 | 0.0454 | 0.1608 | | | | 0.0127 | 0.0069 | 0.0005 | | calc. | 8.1105 | 0.26307 | 15.47 | 13.34 |
| 5§ | T | 0.2352 | 0.0000 | 0.1559 | 0.6030 | 0.0021 | 0.0010 | 0.0027 | | | | 0.0000 | obs. | 8.0891 | 0.26107 | 14.61 | 13.28 |
| | M | 1.6503 | 0.0000 | 0.1065 | 0.1423 | | | | 0.0123 | 0.0067 | 0.0005 | 0.0811 | calc. | 8.0893 | 0.26106 | 14.49 | 13.21 |
| | Total | 1.8855 | 0.0000 | 0.2625 | 0.7453 | 0.0021 | 0.0010 | 0.0027 | 0.0123 | 0.0067 | 0.0005 | 0.0811 | | | | | |
| TS2D 1 | T | 0.1224 | 0.2313 | 0.0000 | 0.6422 | 0.0020 | | 0.0021 | | | | | obs. | 8.1143 | 0.26361 | 15.44 | 13.51 |
| | M | 1.8013 | 0.0068 | 0.0554 | 0.1105 | | | | 0.0190 | 0.0060 | 0.0010 | | calc. | 8.1143 | 0.26361 | 15.42 | 13.50 |
| 2 | T | 0.1319 | 0.2383 | 0.0012 | 0.6245 | 0.0020 | | 0.0022 | | | | | obs. | 8.1138 | 0.26349 | 15.60 | 13.47 |
| | M | 1.7913 | 0.0000 | 0.0552 | 0.1274 | | | | 0.0190 | 0.0062 | 0.0008 | | calc. | 8.1138 | 0.26349 | 15.55 | 13.45 |
| 3 | T | 0.1146 | 0.2076 | 0.0336 | 0.6399 | 0.0021 | | 0.0022 | | | | | obs. | 8.1151 | 0.26348 | 15.61 | 13.47 |
| | M | 1.8081 | 0.0308 | 0.0231 | 0.1120 | | | | 0.0190 | 0.0062 | 0.0008 | | calc. | 8.1151 | 0.26348 | 15.56 | 13.45 |
| 4§ | T | 0.2693 | 0.0000 | 0.1451 | 0.5819 | 0.0019 | | 0.0017 | | | | 0.0000 | obs. | 8.0850 | 0.26073 | 14.29 | 13.22 |
| | M | 1.6265 | 0.0000 | 0.1169 | 0.1425 | | | | 0.0184 | 0.0058 | 0.0010 | 0.0897 | calc. | 8.0854 | 0.26072 | 14.35 | 13.26 |
| | Total | 1.8958 | 0.0000 | 0.2620 | 0.7244 | 0.0019 | 0.0000 | 0.0017 | 0.0184 | 0.0058 | 0.0010 | 0.0897 | | | | | |
| TS2G 1 | T | 0.1191 | 0.2370 | 0.0011 | 0.6394 | 0.0018 | | 0.0016 | | | | | obs. | 8.1136 | 0.26367 | 15.40 | 13.38 |
| | M | 1.8078 | 0.0000 | 0.0494 | 0.1157 | | | | 0.0181 | 0.0067 | 0.0024 | | calc. | 8.1136 | 0.26367 | 15.50 | 13.42 |
| 2 | T | 0.2421 | 0.2024 | 0.0264 | 0.5248 | 0.0021 | | 0.0022 | | | | | obs. | 8.1121 | 0.26176 | 15.56 | 13.50 |
| | M | 1.6806 | 0.0360 | 0.0293 | 0.2272 | | | | 0.0180 | 0.0072 | 0.0018 | | calc. | 8.1121 | 0.26176 | 15.51 | 13.47 |
| 3 | T | 0.2628 | 0.2267 | 0.0000 | 0.5067 | 0.0019 | | 0.0019 | | | | | obs. | 8.1107 | 0.26168 | 15.48 | 13.45 |
| | M | 1.6618 | 0.0111 | 0.0535 | 0.2466 | | | | 0.0180 | 0.0070 | 0.0020 | | calc. | 8.1107 | 0.26168 | 15.50 | 13.46 |

§ Oxidized samples; □ vacancies. Data on unoxidized crystals from Della Giusta *et al.*, 1996

vacancy-free and oxidized spinels in sample TS2 is straightforward.

Al, Mg and $Fe^{3+}$, now present, undergo quite different distributions with respect to vacancy-free spinels. $Fe^{3+}$ (now present in considerable amounts) is similarly distributed between T ($\sim$0.15) and M sites ($\sim$0.10 per f.u.), whereas the low quantities of $Fe^{3+}$ in the natural and heated sample TS2 were only found in the M site. Magnesium distributions do not compare with untreated or heated values, being respectively $\sim$0.60 in T and $\sim$0.14 per f.u. in M sites. Aluminium disorder resembles that of the natural heated sample at 1150°C, $^{[4]}$Al reaching $\sim 0.25 - 0.27$ per f.u..

To summarize, in oxidized spinels:

in the T site, trivalent ions are more abundant than in all the stoichiometric spinels, reaching a total of $\sim$0.40 per f.u.; all the $Fe^{2+}$ of the sample which was then oxidized resided here (contrary to what happens in titanomaghemites; O'Reilly and Banerjee, 1967);

in the M site, cation occupancy is quite different with respect to that at the highest temperature: outgoing Mg is not completely counterbalanced by incoming $Fe^{3+}$. The resulting difference is $\sim 0.08 - 0.09$ vacancies, restricted to the M site, as already found by Guse and Saalfeld (1990), Basso *et al.* (1991), Lucchesi and Della Giusta (1994) and Waerenborgh *et al.* (1994).

In oxidation processes, higher diffusion of $Fe^{3+}$ between the sites is observed, probably due to the presence of vacancies, as already noted by Waerenborgh *et al.* (1994), Larsson *et al.* (1994) and O'Neill *et al.* (1991).

### *Continuity of the series*

The proposed cation distribution leads to clear dependence between the non-fractional oxygen positional parameter $u^* = a \times u$ and the ratio $q(T)/q(M)$ (charge unbalance), where $q(T)$ and $q(M)$ are the charges in T and M sites, respectively (see Fig. 1). The relation between these two parameters is linear:

$$u^* = c_1 \times q(T)/q(M) + c_2 \qquad (15)$$

with $c_1 = -0.428$, $c_2 = 2.293$ and $R^2 = 0.987$.

As charge unbalance is a measure of the number of trivalent cations in the T site, it follows that $u^*$ decreases as trivalent cations enter the T site. This occurs continuously as temperatures become progressively higher and goes further with oxidation. This sequence suggests that oxidation may be regarded as a development of heating.

### *Comparison with other series*

The same clear dependence described by equation (15) is evident (see Fig. 2) working on data on other series in the literature (Larsson *et al.*, 1994; Lucchesi and Della Giusta, 1994; O'Neill *et al.*, 1991; Roelofsen *et al.*, 1992; O'Neill *et al.*, 1992). In series *i* (synthetic $FeAl_2O_4$ ), the $u^*$ decrease on increasing $q(T)/q(M)$ corresponds to increasing temperatures, as in our sample TS2. Series *iii*, *iv* (synthetic $NiAl_2O_4$) and *v* (synthetic $MgFe_2O_4$), which are partially inverse, behave in the opposite way. That is, in both inverse and normal spinels, increasing temperature causes cation distribution to approach $q(T)/q(M) = 0.5$, corresponding to an equal number of charges in the T and in each of the two M sites. Therefore, one hypothesis is that this arrangement represents the 'limit' approached by the spinel structure as temperature approaches infinity. As a matter of fact, at least in binary spinels, $q(T)/q(M) = 0.5$ at $x = 2/3$ ($x$ = degree of inversion), a state corresponding to random distribution and maximum configurational entropy (Navrotsky and Kleppa, 1967).

## Conclusions

The proposed 'addition of oxygen' mechanism, like that used by O'Reilly and Banerjee for titanomaghemites, fits our experimental data of TS2 spinel very well. Cation distributions calculated in the oxidized samples follow the same trend as those in heated samples and correspond to a higher temperature arrangement. The TS2 series behaves like other series in the literature, as regards charge increase in the T site with temperature. To our knowledge, no other series besides TS2, in which cation distribution both on heating and after total oxidation could be followed, has appeared in the literature.

Hematite inclusions, identified in oxidized crystals, were not detectable either by X-ray diffraction or by electron microprobe analysis: their role is marginal in the process described.

Further investigations on cation distributions in spinels oxidized at various temperatures would be informative. It would also be interesting to heat oxidized samples further, to verify whether oxidation also corresponds to the maximum degree of inversion for a given composition.

Lastly, the methods described in this work to study artificially oxidized spinels (single-crystal X-ray structural refinement, electron microprobe analysis, cation distribution calculated assuming vacancies or otherwise) may also be adopted to study natural, possibly non-stoichiometric, spinels.

## Acknowledgements

This work was supported by the Italian Consiglio Nazionale delle Ricerche (CNR Centro di Studio per la Geodinamica Alpina, Padova) and the Ministero

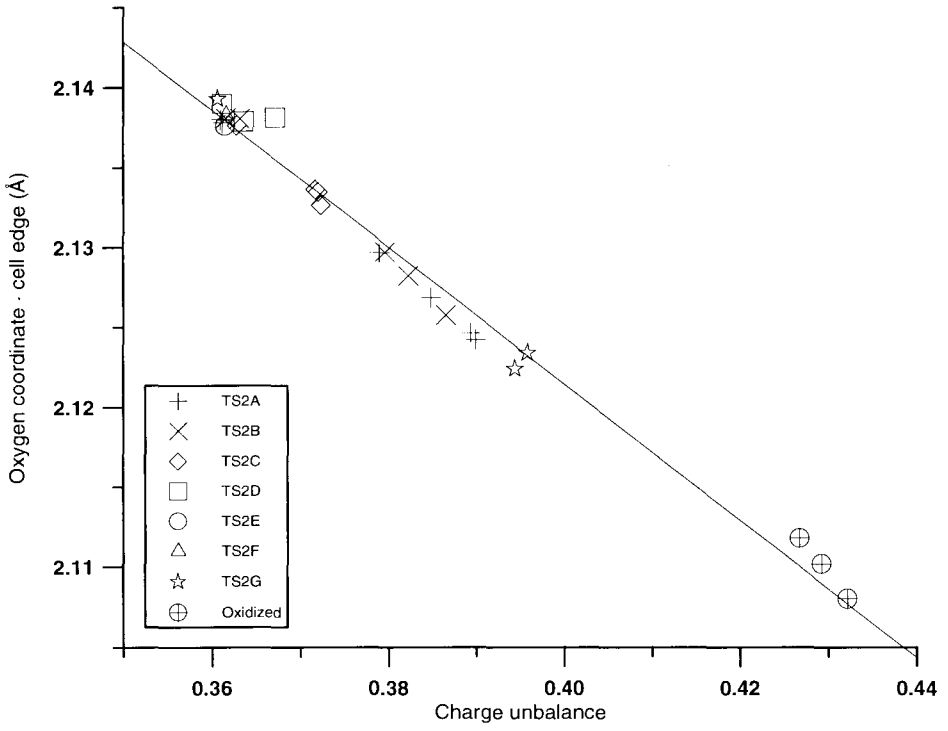


FIG. 1. Plot of $u^* = u \times a$ against charge unbalance in TS2 sample. Oxidized samples on far right. Note clear continuity of all crystals in series up to oxidized samples.

dell'Università e della Ricerca Scientifica e Tecnologica. Raoul Carampin kindly assisted in the microanalysis. The authors are grateful to Prof. G. Fagherazzi for his reading of the manuscript, and to Ms G. Walton for revision of the English text.

## References

Basso, R., Carbonin, S. and Della Giusta, A. (1991) Cation and vacancy distribution in a synthetic defect spinel. *Zeit. Kristallogr.*, **194**, 111–9.

Blessing, R.H., Coppens, P. and Becker, P. (1972) Computer analysis of step-scanned X-ray data. *J. Appl. Crystallogr.*, **7**, 488–92.

Carbonin, S., Russo, U. and Della Giusta, A. (1996) Cation distribution in some natural spinels from X-ray diffraction and Mössbauer spectroscopy. *Mineral. Mag.*, **60**, 355–68.

Clegg, W. (1981) Faster data collection without loss of precision. An extension of the learnt profile method. *Acta Crystallogr.*, **A37**, 22–28.

Colombo, U., Fagherazzi, G., Gazzarrini, F., Lanzavecchia, G. and Sironi, G. (1964*a*) Studio sull'ossidazione delle magnetiti. *Chimica e Industria*, **46**, 357–62.

Colombo, U., Fagherazzi, G., Gazzarrini, F., Lanzavecchia, G. and Sironi, G. (1964*b*) Mechanisms in the first stage of oxidation of magnetites. *Nature*, **202**, 175–6.

Comin-Chiaramonti, P., Demarchi, G., Siena, F. and Sinigoi, S. (1982) Relazioni tra fusione e deformazione nella peridotite di Balmuccia (Ivrea-Verbano). *Rend. Soc. Ital. Mineral. Petrol.*, **38**, 685–700.

Davis, B.L., Rapp, G.Jr. and Walawender, M.J. (1968) Fabric and structural characteristics of the martitization process. *Amer. J. Sci.*, **266**, 482–96.

Della Giusta, A., Carbonin, S. and Ottonello, G. (1996) Temperature-dependent disorder in a natural Mg-Al-$Fe^{2+}$-$Fe^{3+}$-spinel. *Mineral. Mag.*, **60**, 603–16.

Feitknecht, W. and Gallagher, K.J. (1970) Mechanisms for the oxidation of $Fe_3O_4$. *Nature*, **228**, 548–9.

Fleet, M.E. and Arima, M. (1985) Oriented hematite inclusions in sillimanite. *Amer. Mineral.*, **70**, 1232–7.

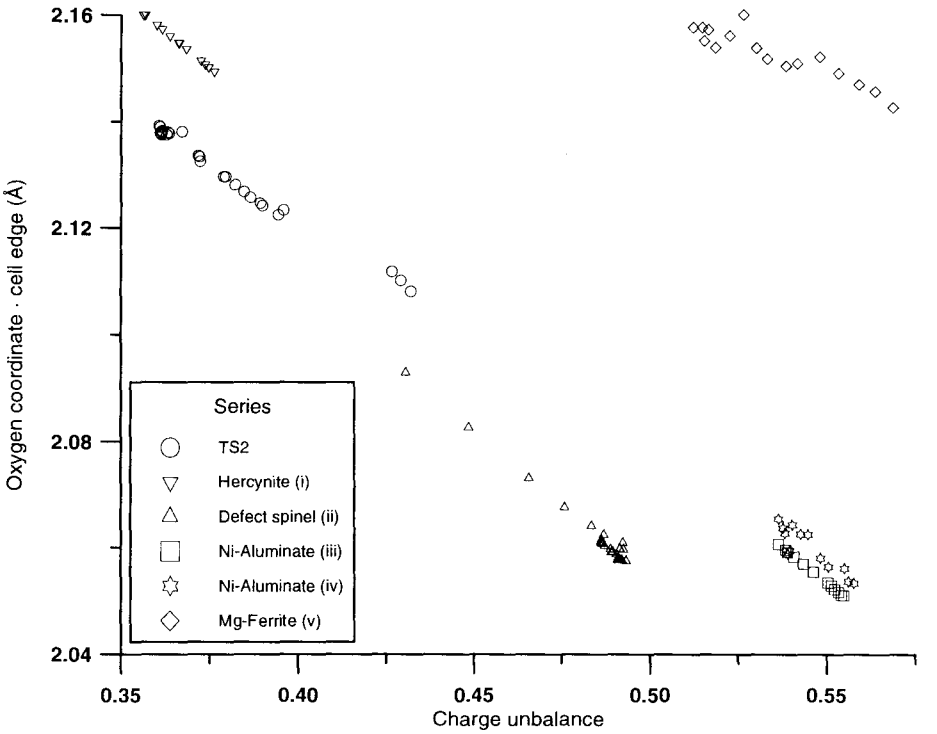


FIG. 2. Correlations between $u^* = u \times a$ and charge unbalance in several published series. In series *i*, *ii*, and *iii*, cation distributions and crystallographic parameters were recalculated from literature data (see section on model used for cation distribution calculation). In series *iv* and *v*, data were used as published.
N.B.: $q(T)/q(M) = 0.5$ means equal charges in the T and in two M sites; regions respectively left and right of 0.5 correspond to normal and inverse spinels; left of 0.5, inversion degree increases with temperature; right of 0.5 it decreases; in all cases, on increasing temperature, series approach $q(T)/q(M) = 0.5$ which, for binary spinels, corresponds to $x = 2/3$, and to maximum disorder and configurational entropy.

Guse, W. and Saalfeld, H. (1990) X-ray characterization and structure refinement of a new cubic alumina phase ($\sigma$-$Al_2O_3$) with spinel-type structure. *Neues Jahrb. Mineral., Mh.*, 217–26.

Hill, R.J., Craig, J.R. and Gibbs, G.V. (1979) Systematics of the spinel structure type. *Phys. Chem. Minerals*, **4**, 317–39.

James, F. and Roos, M. (1975) MINUIT. A system for function minimization and analysis of the parameters errors and correlations. *Comp. Phys. Comm.*, **10**, 343–67.

Kullerud, G., Donnay, G. and Donnay, J.D.H. (1969) Omission solid solution in magnetite: Kenotetrahedral magnetite. *Zeit. Kristallogr.*, **128**, 1–17.

Larsson, L., O'Neill, H.St.C. and Annersten, H. (1994) Crystal chemistry of synthetic hercynite ($FeAl_2O_4$) from XRD structural refinements and Mössbauer spectroscopy. *Eur. J. Mineral.*, **6**, 39–51.

Lucchesi, S. and Della Giusta, A. (1994) Crystal chemistry of non-stoichiometric Mg-Al synthetic spinels. *Zeit. Kristallogr.*, **209**, 714–9.

Navrotsky, A. and Kleppa, O.J. (1967) The thermodynamics of cation distribution in simple spinels. *J. Inorg. Nucl. Chemistry*, **29**, 2701–14.

Navrotsky, A., Wechsler, B.A., Geisinger, K. and Seifert, F. (1986) Thermochemistry of $MgAl_2O_4$-$Al_{8/3}O_4$ defect spinels. *J. Amer. Ceramic Soc.*, **69**, 418–22.

North, A.C.T., Phillips, D.C. and Scott-Mattews, F. (1968) A semi-empirical method of absorption correction, *Acta Crystallogr.*, **A24**, 351–2.

O'Neill, H.St.C., Dollase W.A. and Ross, C.R.II (1991) Temperature dependence of the cation distribution in Nickel Aluminate ($NiAl_2O_4$) spinel: a powder XRD study. *Phys. Chem. Minerals*, **18**, 302–19.

O'Neill, H.St.C., Annersten, H. and Virgo, D. (1992) The temperature dependence of the cation distribution in magnesioferrite ($MgFe_2O_4$) from powder XRD structural refinements and Mössbauer spectroscopy. *Amer. Mineral.*, **77**, 725–40.

O'Reilly, W. and Banerjee, S.K. (1967) The mechanism of oxidation in titanomagnetites: a magnetic study. *Mineral. Mag.*, **36**, 29–37.

Pizzolon, M. (1991) *Cristallochimica e modellizzazione di spinelli di Mg–Al–Fe–Cr.* Thesis, University of Padova, Padova, Italy.

Princivalle, F., Della Giusta, A. and Carbonin, S. (1989) Comparative crystal chemistry of spinels from some suites of ultramafic rocks. *Mineral. Petrol.*, **40**, 117–26.

Roelofsen, J.N., Peterson, R.C. and Raudsepp, M. (1992) Structural variation in nickel aluminate spinel ($NiAl_2O_4$). *Amer. Mineral.*, **77**, 522–8.

Sheldrick, G.M. (1993) *SHELX-93. Program for crystal structure refinement.* University of Göttingen, Germany.

Viertel, H.U. and Seifert, F. (1979) Physical properties of defect spinels in the system $MgAl_2O_4$-$Al_2O_3$. *Neues Jahrb. Mineral., Abh.*, **134**, 167–82.

Waerenborgh, J.C., Figuereido, M.O., Cabral, J.M.P. and Pereira, L.C.J. (1994) Powder XRD structure refinements and $^{57}Fe$ Mössbauer effect study of synthetic $Zn_{1-x}Fe_xAl_2O_4$ ($0< x \leqslant 1$) spinels annealed at different temperatures. *Phys. Chem. Minerals*, **21**, 460–8.

[*Manuscript received 15 March 1996: revised 16 September 1996*]